Accelerated UV treatment of Carbamazepine and NDMA in water under 222 nm irradiation

Bryan Liu, Lauren Mullen, Emma M. Payne, Karl G. Linden*

Department of Civil, Environmental, and Architectural Engineering, University of Colorado Boulder, 4001 Discovery Dr., Boulder, CO, 80303, United States

* Corresponding Author: karl.linden@colorado.edu

Abstract

Krypton Chloride (KrCl*) excimer ultraviolet (UV) light may provide advantages for contaminant degradation compared to conventional low-pressure (LP) UV. Direct and indirect photolysis as well as UV/hydrogen peroxide driven advanced oxidation (AOP) of two chemical contaminants were investigated in laboratory-grade water (LGW) and treated secondary effluent (SE) for LPUV and filtered KrCl* excimer lamps emitting at 254 and 222 nm, respectively. Carbamazepine (CBZ) and *N*-Nitrosodimethylamine (NDMA) were chosen based on their unique molar absorption coefficient profiles, quantum yields (QY) at 254 nm, and reaction rate constants with hydroxyl radical. Quantum yields and molar absorption coefficients at 222 nm for both CBZ and NDMA were determined with the molar absorption coefficient measured to be 26,422 and 8,170 $M^{-1}cm^{-1}$, respectively and the, QY determined as 1.95×10^{-2} and 6.68×10^{-1} mol Es^{-1}, respectively. 222 nm irradiation of CBZ in SE improved degradation compared to LGW, likely through promotion of in-situ radical formation. AOP conditions improved degradation of CBZ in LGW for both UV LP and KrCl* sources but did not improve NDMA decay. In SE, photolysis of CBZ resulted in similar decay as AOP, likely due to the in-situ generation of radicals. Overall, KrCl* 222 nm source significantly improves contaminant degradation over 254 nm LPUV.

Keywords: LPUV, KrCl* excimer, UV/AOP, peroxide, photolysis, UV light

Synopsis:

222 nm photolysis and advanced oxidation greatly improve the degradation of carbamazepine and NDMA in water compared to conventional 254 nm UV.

Graphical Abstract

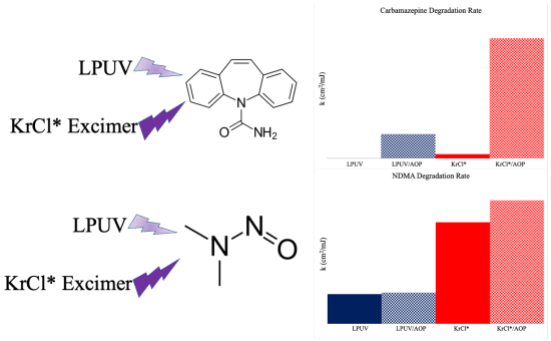

1. Introduction

UV and UV advanced oxidation processes (UV/AOPs) are widely used in the water/wastewater treatment industry[1–4]. Conventional UV sources include low-pressure (LP) UV lamps, which emit a monochromatic light at 254 nm. Several compounds degrade effectively through direct photolysis, such as ketoprofen and *N*-Nitrosodimethylamine (NDMA)[2,5], while others degrade through •OH driven AOP, such as carbamazepine (CBZ) and 1,4-dioxane[5–8].

Despite its effectiveness, several drawbacks pertain to LPUV, such as the potential for mercury contamination, damage to skin and eyes in cases of accidental exposure, and the time to ignition needed before usage[9–11]. A lamp source emerging into the market is KrCl* excimer lamps. KrCl* excimer lamps emit light primary at 222 nm, in the loosely-defined Far-UVC range (200-230 nm). Light emission in the Far-UVC range has been shown to be more efficient at inactivation of viruses and unlikely to be a risk to human skin and eyes when exposed[10,11]. However, little research has investigated the potential of Far-UVC irradiation in water treatment, as a UV/AOP. Two factors affect the direct photolysis degradation of chemical contaminants: 1) absorbance and 2) QY. The absorbance reflects the likelihood of the chemical compound's ability to absorb photons, whereas the QY reflects the efficiency of a chemical transformation upon photon absorbance. The alignment of light emission wavelength, molar absorption coefficient, and high photon energy will generally improve chemical degradation rate constants. In Figure 1, the molar absorption coefficient of CBZ and NDMA are shown along with the relative light emission (RLE) of LPUV at 254 nm and KrCl* excimer lamp at 222 nm. CBZ and NDMA both absorb significantly higher at 222 nm compared to 254 nm, indicating that more photons will be absorbed in the Far-UVC range, likely improving degradation through direct photolysis.

UV-based AOPs may also be benefit from utilizing filtered KrCl* excimer lamps. AOPs are driven by the formation of •OH, which are highly reactive and non-selective with many organic and inorganic compounds[12]. Contaminants, such as CBZ, which degrades negligibly under direct photolysis, degrades significantly faster through AOPs due to its fast reaction rate with •OH $\left(k_{\bullet OH/CBZ} = 8.02 \times 10^9\ M^{-1}s^{-1}\right)$[13]. UV/AOP is a commonly used process in water/wastewater treatment[14–16]. While the most commonly used •OH promoter is hydrogen peroxide (H_2O_2) advanced oxidation can also be achieved by coupling UV with nitrate, iron, persulfate, and free chlorine [1,17–21]. UV/H_2O_2 has been widely used and is very effective in treating numerous target contaminants. As illustrated in Figure 1, the molar absorption coefficient of H_2O_2 overlaps minimally with LPUV emission but has a higher absorbance in the Far-UVC range, indicating that a higher formation rate or steady-state concentration of •OH is possible under Far UVC.

Background water matrices are known to inhibit the process efficiency of UV-based advanced oxidation. This can be attributed to light screening and •OH scavenging by dissolved organic matter (DOM), alkalinity, and nitrate/nitrite[22,23]. Pereira et al. (2007) showed that LPUV with the addition of 10 mg/L of H_2O_2 was able to improve the degradation of CBZ and naproxen by 545- and 50-fold in lab grade water, respectively, but in surface water, the improvement was only 90- and 6-fold, respectively. A study by Lee et al. (2020) concluded that high level of nitrate curbed the removal rate of the target contaminant significantly in a LPUV system.

Recent interest in Far UVC disinfection of viruses[24–26] and the testing of KrCl* lamps in field studies[11,27] motivated an investigation of the potential benefits of KrCl* excimer lamps for UV/AOP. The goal of this study was to compare the degradation efficacy of target contaminants between KrCl* excimer lamps that emit photons primarily at 222 nm and LPUV that emit photons

at 254 nm. The specific scope included 1) determining fundamental photolysis parameters (absorbance and quantum yield) in lab grade water for the chosen chemicals under 222 filtered excimer lamps; 2) measuring the formation of hydroxyl radicals in the Far-UVC range and the steady-state hydroxyl radical concentration in field water; and 3) evaluating the degradation efficiency of target contaminants in both lab and field water. CBZ and NDMA were selected as target contaminants for this study because they complement each other with regard to their differences in rates of photolysis and •OH oxidation.

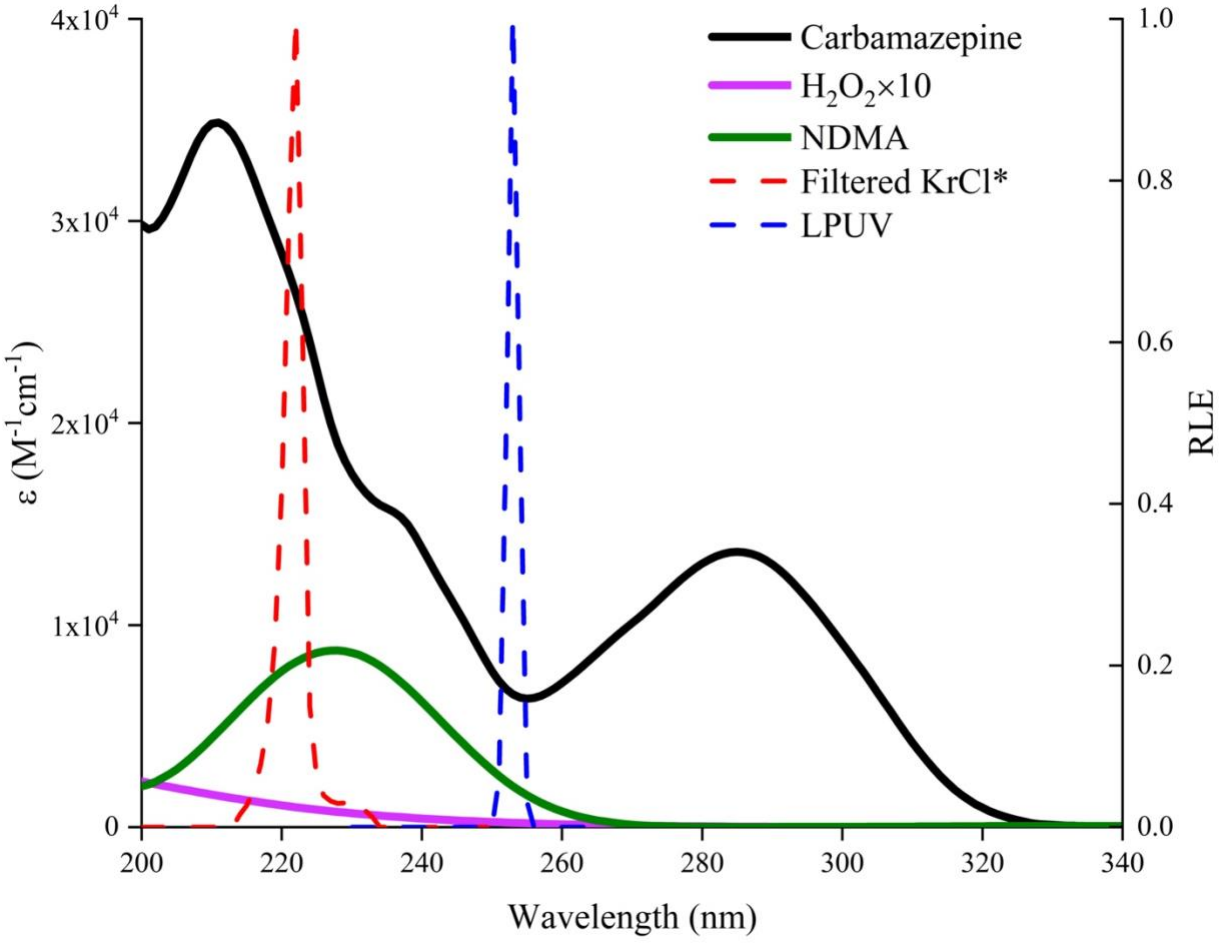

Figure 1. Molar absorption spectra of CBZ, NDMA, and H_2O_2 (×10), and emission spectra of excimer 222 filtered and LPUV sources

2. Materials and Methods

2.1 UV exposure experiments

UV lamps were set up in a bench-scale collimated beam apparatus. Two lamp types were investigated during this study: a KrCl* excimer lamp emitting primarily at 222 nm (USHIO, Cypress, CA, USA), and four conventional LP mercury lamp emitting at 254 nm (15 watts each, #G15T8, USHIO). KrCl* excimer emits primarily at 222 nm with a small peak at 258 nm. A bandpass filter was applied to isolate only the irradiation around 222 nm, denoted as filtered KrCl* excimer. Incident UV irradiance was measured using a calibrated radiometer and sensor (Model ILT5000, Model SED240, International light Inc.). The average irradiance was determined by correcting the incident irradiance for sample depth, absorbance at 254 nm, water factor, reflection factor, divergence factor, and petri factor [28]. A small stir bar was added in the water sample to induce good mixing without disturbing the water surface. Dark controlled experiments were performed for CBZ and NDMA with and without the addition of H_2O_2 to confirm no degradation of the compounds occurred. Loss of concentration was not observed in stirred samples placed in the dark. The starting concentrations for CBZ and NDMA were both 1 mg/L.

2.2 Chemical selection

CBZ and NDMA were selected as target contaminants for this study based on their unique photochemical and physio-chemical properties at 254 nm. At 254 nm, CBZ degrades slowly through direct photolysis, due to a low quantum yield of ($\Phi_{CBZ} = 6 \times 10^{-4}$ mol/Es)[13] ,however, it has a fast second order reaction rate with •OH ($k_{\bullet OH/CBZ} = 8.08 \times 10^{9}\ M^{-1}s^{-1}$), which is the main pathway for its degradation. In contrast, the main pathway for NDMA degradation is photolysis. NDMA has a significantly higher quantum yield ($\Phi_{NDMA} = 0.25$ mol/Es) and

relatively low second order reaction rate with •OH ($k_{\bullet OH/NDMA} = 3.30 \times 10^8\ M^{-1}s^{-1}$), resulting in photolysis as its main degradation pathway [13]. Chemical structures of CBZ and NDMA can be seen in Supporting Information (SI) Figure S1 and S2, respectively.

2.3 Reagents and test waters

Analytical grade CBZ and NDMA were purchased from Sigma-Aldrich and Fisher Scientific, respectively, and used without further purification. All stock solutions, chemicals, H_2O_2 were prepared in LGW ($\text{resistance} = 18M\Omega\ \text{cm}$). 0.5mM of sodium carbonate was used to maintain the sample at approximately pH 7 for all exposures conducted in LGW. pH values for each water before and after UV treatment are presented in Tables S1 and S2 in the Supporting Information. Secondary effluent (SE) was collected from a non-RO based pilot water reuse treatment train from a Water Reclamation Facility in Oklahoma. The wastewater was treated with ozonation and biological aerated filtration (ozone/BAF) before collection for use in this study. Measured water quality parameters for the SE are presented in Table 3.

2.4 Analytical methods

A Cary 4000 UV-vis spectrophotometer was used to measure UV absorption. Residual H_2O_2 was measured using the I_3^- method [29]. Organic carbon was measured using a Sievers M5310C TOC analyzer. Alkalinity was measured using a HACH digital titrator. Nitrate and nitrite were measured using HACH TNT 840 and TNT 839 test vials, respectively, in a HACH DR6000 spectrophotometer.

CBZ, and NDMA were detected using an Agilent 1220 Series HPLC with UV-vis detection. The HPLC consisted of a reverse phase C-18 column and UV-vis detector. An eluent consisting of 50% acetonitrile: 50% ultrapure water and UV-vis detection at 286 nm was used for CBZ. An eluent

consisting of 15% methanol: 85% ultrapure water and UV-vis detection at 230 nm was used for NDMA.

3. Results and Discussion

3.1 UV and UV/AOP in LGW

Table 1. CBZ and NDMA fluence-based degradation rate constants for filtered 222 nm excimer lamp and LPUV for both direct photolysis and UV/AOP (10ppm H_2O_2)

	Direct Photolysis (cm^2/mJ)		**AOP ($10ppm\ H_2O_2$) (cm^2/mJ)**	
	Excimer 222F	**LPUV**	**Excimer 222F**	**LPUV**
CBZ	$(9.49 \pm 0.23) \times 10^{-4}$	$(4.33 \pm 1.38) \times 10^{-5}$	$(2.58 \pm 0.08) \times 10^{-2}$	$(5.24 \pm 0.16) \times 10^{-3}$
NDMA	$(2.18 \pm 0.02) \times 10^{-2}$	$(6.36 \pm 0.05) \times 10^{-3}$	$(2.65 \pm 0.3) \times 10^{-2}$	$(6.71 \pm 0.25) \times 10^{-3}$

Direct photolysis and AOP for both CBZ (Figure 2A) and NDMA (Figure 2B) were investigated under both filtered KrCl* excimer and LPUV lamp. The degradation rate constants under each system are summarized in Table 1. Degradation of CBZ significantly improved under both direct photolysis and AOP when utilizing filtered KrCl* excimer compared to LPUV. The degradation rate constant is approximately 21 times and 5 times faster under filtered KrCl* excimer compared to LPUV for both direct photolysis and AOP, respectively. The addition of 10 mg/L of H_2O_2 significantly improved the degradation of CBZ under both filtered KrCl* excimer and LPUV. Interestingly, the additional degradation due specifically to AOP (by subtracting the degradation rate constant of direct photolysis), was quite different between the KrCl* and LPUV AOP. The

degradation rate constant of CBZ solely due to AOP is 5.20×10^{-3} cm^2/mJ for LPUV, whereas the degradation rate constant is 2.49×10^{-2} cm^2/mJ for filtered KrCl* excimer lamp AOP, indicating 4.8 times better performance for filtered KrCl* excimer lamp under •OH oxidation. This enhancement is likely due to the higher molar absorption coefficient of H_2O_2 at 222 nm compared to 254 nm.

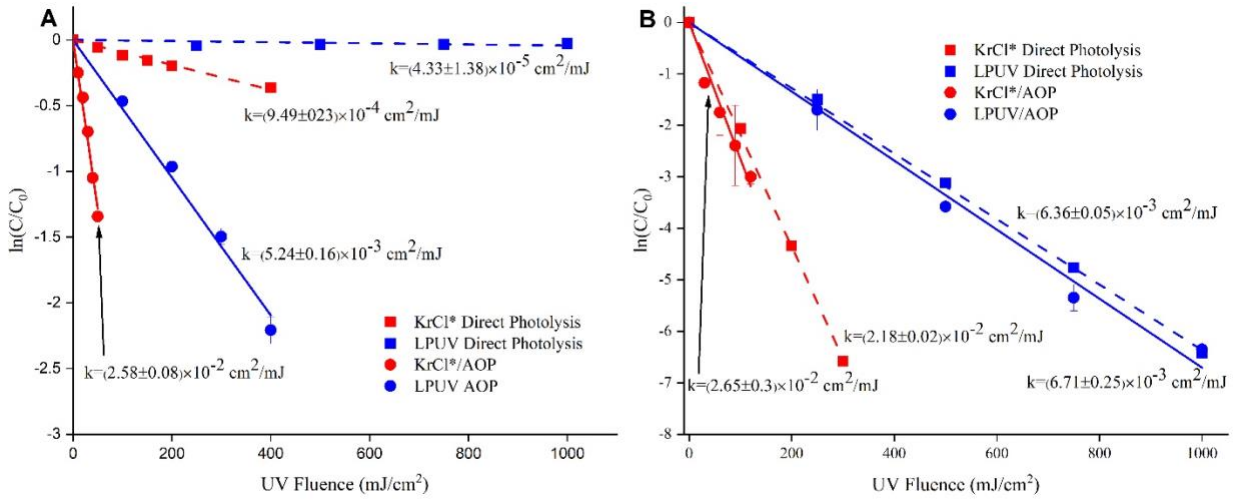

Figure 2. Comparison of A) CBZ and B) NDMA degradation between filtered 222 nm excimer lamp and LPUV under both direct photolysis (square) and UV/AOP (10ppm H_2O_2) (circle) in LGW

The degradation of NDMA through direct photolysis was relatively fast under LPUV, as expected from previous studies due to its high quantum yield at 254 nm, but filtered KrCl* excimer increased the degradation of NDMA by approximately 3.5-fold. Degradation of NDMA did not improve for either LPUV nor filtered KrCl* excimer lamp with the addition of 10 mg/L of H_2O_2. This aligns with theoretical predictions: NDMA already has high a QY and reacts relatively slow with •OH ($k_{\bullet OH/NDMA} = 3.30 \times 10^8$ $M^{-1}s^{-1}$). AOP not resulting in improving the degradation of NDMA is evident in multiple other studies [2,18,30].

158 The significant improvement of direct photolysis and/or AOP for contaminant degradation at 222
159 nm compared to 254 nm can be explained by the combination of absorbance and QY. Absorbance
160 is the likelihood of a photon being absorbed by a molecule, and photochemical reactions can only
161 occur if photons are being absorbed[31]. The second factor is the quantum yield of a chemical, which
162 is defined as the net change of a chemical concentration per Einstein of photons absorbed[32].

163 Limited studies have been performed in the Far-UVC range to date, and little to no information is
164 available for either CBZ or NDMA. The molar absorption coefficient, ε, is determined using Beer-
165 Lambert Law as shown in Eqn. (1).

166 $$\varepsilon = \frac{A}{lC} \quad (1)$$

167 Where A is the absorbance of the sample at a particular pathlength, ε is the molar absorption
168 coefficient ($M^{-1}cm^{-1}$), l is the pathlength, and C is the concentration of the target compound (M).
169 In this study, up to two different concentrations of CBZ and NDMA were made to determine the
170 molar absorption coefficient.

171 The QY under LPUV and filtered KrCl* excimer lamp is determined using Eqn. 2[31].

172 $$\Phi = \frac{10}{\ln(10)} \frac{k_1}{PF \int_{\lambda_1}^{\lambda_2} \varepsilon(\lambda)\, E_{p,\lambda}^0 [RF(\lambda)][WF(\lambda)] d\lambda} \quad (2)$$

173 Where Φ is the quantum yield, k_1 is the first order rate constant, PF is the petri factor, ε(λ) is the
174 molar absorption coefficient at wavelength λ, $E_{p,\lambda}^0$ is the incident photo irradiance at the centre of
175 the water surface, RF(λ) is the reflection factor at wavelength λ, WF(λ) is the water factor at
176 wavelength λ.

Figure 1 demonstrates the overlapping of CBZ, NDMA, and H_2O_2 molar absorption coefficient between 200 and 350 nm, as well as the relative light emission (RLE) for filtered KrCl* excimer and LPUV lamps. Both CBZ and NDMA absorb relatively low at 254 nm, which LPUV emission occurs, but much higher at 222 nm, at which filtered KrCl* excimer lamps emission occurs. Values of molar absorption coefficient for CBZ and NDMA can be seen in Table 2. Compared to 254 nm, the molar absorption coefficient of CBZ and NDMA is 4.1 and 4.5 times higher at 222 nm, respectively.

For CBZ, two separate absorbance peaks are observed in Figure 1. The different absorbance value at 222 nm compared to 254 nm is likely due to the different functional groups in CBZ. While UV_{254} is highly correlated with aromatic compounds[33,34], the absorbance peak at 222 nm is likely the result of the amide group. Storozhok and Medyanik (2018) showed that the amide group exhibits an absorption maxima in the Far-UVC range. The difference in absorbance maxima due to different moieties will likely result in different pathways for photolysis-driven CBZ degradation. Since aromatic rings are the dominant absorber of photons at 254 nm, it is likely the main degradation pathway is through photons attacking the aromatic rings which would be consistent with other studies that demonstrated the decrease of aromaticity during UV irradiation[33,36]. As for irradiation at 222 nm, it is likely the degradation pathway is photons attacking the amide group in addition to the aromatic rings. This would be consistent with disinfection studies within the Far-UVC range. KrCl* excimer disinfection studies have demonstrated that protein damage is the main mechanism at 222 nm [25,37,38].

Table 2 also presents quantum yield of CBZ and NDMA for both filtered KrCl* excimer and LPUV. At 254 nm, the QY of CBZ and NDMA was determined to be 1.41×10^{-3} and 0.33 mol/Es, respectively. At 222 nm, an increase in QY was observed for both compounds. The

QY for CBZ and NDMA at 222 nm was determined to be 1.95×10^{-2} and 0.668 mol/Es, respectively.

To achieve contaminant degradation, electrons in the bonding (π) and non-bonding (n) state need to reach the anti-bonding state ($\pi \rightarrow \pi^* \; or \; n \rightarrow \pi^*$)[39]. Not all excited molecules will undergo a photochemical reaction and the rate of a photochemical reaction is proportional to the absorbed photon flux. At equal incident irradiance, KrCl* excimer will emit higher flux of photon compared to LPUV, however, the KrCl* excimer intensity used for this research was 1/5 of LPUV's intensity, resulting in an photon irradiance of 4.64×10^{-7} mEs cm^{-2} s^{-1} at 222 nm compared to 3.16×10^{-6} mEs cm^{-2} s^{-1} at 254 nm, approximately a magnitude lower. However, CBZ still degraded much faster under filtered KrCl* excimer, and this is likely to be attributed to both the absorbance of moieties and their bond enthalpies. As discussed previously, the main absorber at 254 nm is the aromatic rings ($\mathrm{C=C}$), whereas at 222 nm, the main absorber is the primary amide group ($\mathrm{RCONH_2}$). The bond enthalpies of $\mathrm{C=C}$ is 612 kJ/mol, but it is only 306 kJ/mol for $\mathrm{C-N}$, coupled with higher photon energy at 222 nm compared to 254 nm, indicating the degradation of CBZ is likely due to the cleavage of the amide group when irradiated at 222 nm.

The degradation of CBZ by AOP alone was significantly higher for filtered KrCl* excimer lamp than LPUV, implying that there was significantly higher •OH formation at 222 nm than 254 nm, which may be explained by the higher absorbance of $\mathrm{H_2O_2}$ in the Far-UVC range. As shown in Figure 1, $\mathrm{H_2O_2}$ absorbs poorly at 254 nm ($\varepsilon_{\mathrm{H_2O_2}} = 19\ \mathrm{M^{-1}cm^{-1}}$), where at 222 nm, molar absorption coefficient of $\mathrm{H_2O_2}$ increase by approximately 4-fold ($\varepsilon_{\mathrm{H_2O_2}} = 99\ \mathrm{M^{-1}cm^{-1}}$). The quantum yield •OH remains at 1 per mole of $\mathrm{H_2O_2}$ regardless of wavelength, but the increased molar absorption coefficient will result in a higher formation rate of •OH. CBZ was used both as

a target contaminant as well as a •OH probe compound due to its slow photolysis rate and fast second order reaction rate with •OH. Since there are no other scavengers present in the water and CBZ is the predominant species in the water, the formation rate of •OH will be directly related to the degradation rate of CBZ solely due to AOP [40].

This is also evident in the degradation of H_2O_2. As shown in Supporting Information Table S1and S2 for H_2O_2 concentration in CBZ and NDMA experiments, respectively, H_2O_2 concentration decreases substantially more in the filtered KrCl* excimer experiments than the LPUV experiments. For CBZ degradation in LGW, H_2O_2 concentration decreased from 9.49 ppm to 9.00 ppm over a UV fluence of 400 mJ/cm^2 in the LPUV system, while H_2O_2 concentration decreased from 9.16 ppm to 8.21 ppm over a UV fluence of 40 mJ/cm^2 in the filtered KrCl* excimer system. This indicates that for every mJ/cm^2 of LPUV fluence, 0.0012 ppm of H_2O_2 is utilized, while 0.0238 ppm of H_2O_2 is utilized for every mJ/cm^2 of KrCl* UV fluence. Similar results were obtained from NDMA in LGW experiments. H_2O_2 concentration decreased from 9.61 ppm to 8.27 ppm over a UV fluence of 1000 mJ/cm^2 for LPUV, while H_2O_2 concentration decreased from 9.61 ppm to 9.18 ppm over a UV fluence of 120 mJ/cm^2 in the filtered KrCl* excimer system, indicating that for every mJ/cm^2 of LP UV fluence, 0.0013 ppm of H_2O_2 is utilized, while 0.0036 ppm of H_2O_2 is utilized for every mJ/cm^2 of KrCl* UV fluence.

Table 2. Comparison of CBZ and NDMA molar absorption coefficient and quantum yield for filtered KrCl* excimer and LPUV

Chemical	ε_{254} $M^{-1}cm^{-1}$	Φ_{254} mol Es^{-1}	ε_{222} $M^{-1}cm^{-1}$	Φ_{222} mol Es^{-1}
CBZ	6419 ± 118	1.41×10^{-3}	26422 ± 246	1.95×10^{-2}
NDMA	1799 ± 106	0.33	8170 ± 266	0.668

3.2 UV and UV/H_2O_2 in Secondary Effluent

Background water constituents (e.g., DOC, carbonate, nitrate, etc.) can have major impacts on the water absorption as well as a scavenging effect on radical formation. Table 3 shows the major water quality parameters from a secondary effluent used in this study. The water has low TOC concentration (3.5 mgC/L) but high alkalinity (194 mg$CaCO_3$/L), and a nitrate concentration of 1.75 mgN/L. The absorbance increased by 15 fold between 254 to 222 nm; from 0.029 cm^{-1} at 254 nm, to 0.447 cm^{-1} at 222 nm. The significant increase is likely due to the increased absorbance of TOC and nitrate in the Far-UVC range.

Table 3. Water quality of ozone/BAF treated secondary effluent used in this study

Parameter	Value
$\mathrm{TOC\ (mg/L)}$	3.50 ± 0.04
$\mathrm{Alkalinity\ (mgCaCO_3/L)}$	194
pH	7.63
$\mathrm{NO_3^-\ (mgN/L)}$	1.75
$\mathrm{NO_2^-\ (mgN/L)}$	0.055
$\mathrm{A_{254nm}\ (cm^{-1})}$	0.028
$\mathrm{A_{222nm}\ (cm^{-1})}$	0.427

Figure 3 shows the degradation of CBZ (Figure 3A) and NDMA (Figure 3B) for both direct photolysis and AOP under filtered KrCl* excimer and LPUV, and the degradation rate constants are presented in Table 4. Filtered KrCl* excimer lamp was able to significantly improve the degradation rate constant of CBZ compared to LPUV for both direct photolysis and AOP. In the LPUV system, the addition of H_2O_2 significantly improved CBZ degradation but the same effect

was not observed under filtered KrCl* excimer lamps. This might be due to various factors explained below.

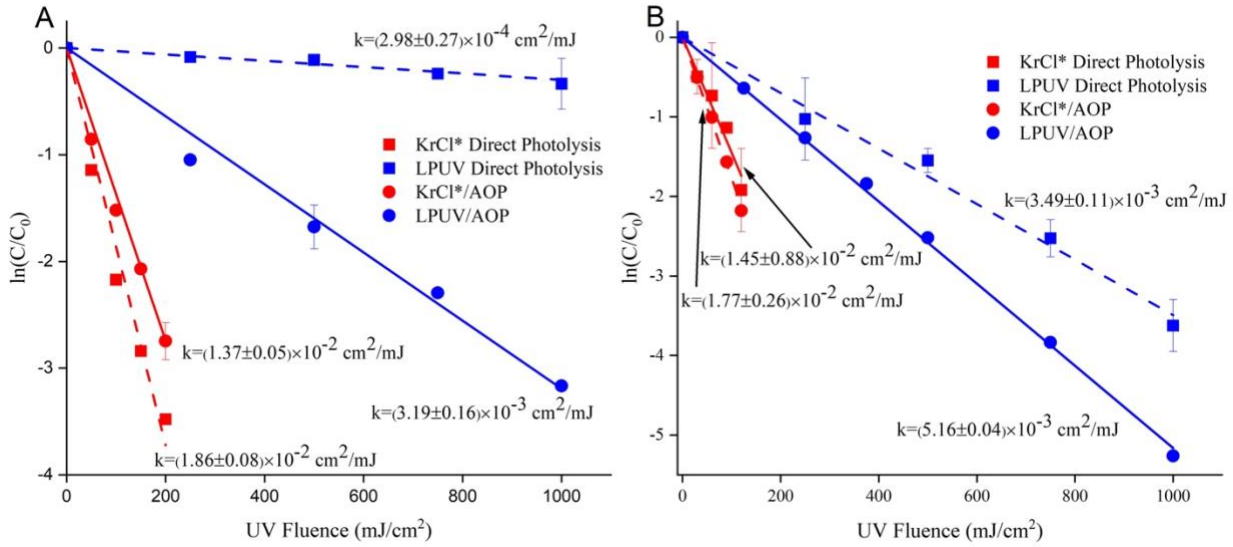

Figure 3. Comparison of A) CBZ and B) NDMA degradation between filtered KrCl* excimer lamp and LPUV under both direct photolysis (square) and UV/AOP (10ppm H2O2) (circle) in SE

The degradation results of NDMA in SE reflected the results obtained in LGW, for both LPUV and filtered KrCl* excimer lamp. Direct photolysis of NDMA under filtered KrCl* lamp improved by 4.1-fold compared to LPUV. The addition of 10 mg/L of H_2O_2 did not improve NDMA degradation for either filtered KrCl* lamp nor LPUV.

The degradation rate constants of CBZ and NDMA in SE were quite different to that of in LGW. For CBZ, direct photolysis of LPUV and KrCl* excimer lamp in SE improved the degradation by 6.9 and 19.6 times compared to LGW, respectively, whereas the degradation rate constant of LPUV/H_2O_2, and $KrCl^*/H_2O_2$ was higher in LGW than SE by about 1.8 and 1.7 times, respectively. Unlike the results in LGW, direct photolysis of CBZ by filtered KrCl* excimer lamp was more efficient than LPUV/H_2O_2 in SE. This may be due to radicals formed in situ from background water constituents. With background absorbance being 15-fold higher at 222 nm

compared to 254 nm, it is likely that appreciable concentrations of radicals were formed from organic matter, nitrate, and/or carbonate in the water, including singlet oxygen, •OH, and reactive nitrogen species, which may all have contributed to CBZ degradation[41,42]. For NDMA, the degradation rate constant under LPUV, LPUV/H_2O_2, KrCl* excimer lamp, and $KrCl^*/H_2O_2$ systems decreased by 50, 20, 30, and 30% in SE compared to LGW, respectively. The decrease of NDMA degradation rate constant in SE compared to LGW for all UV systems is most likely due to light screening since background absorbance increased by 15-fold, and AOPs play minimal role in NDMA degradation process.

Similar to the results in LGW, H_2O_2 concentration decreased at a significantly higher rate under filtered KrCl* excimer lamp than LPUV, as shown in Table S1 and S2 for H_2O_2 concentration in CBZ and NDMA experiments, respectively. For CBZ degradation in SE, H_2O_2 concentration decreased from 9.99 ppm to 8.85 ppm over a UV fluence of 1000 mJ/cm^2 in the LPUV system, while H_2O_2 concentration decreased from 10.00 ppm to 6.41 ppm over a UV fluence of just 200 mJ/cm^2 in the filtered KrCl* excimer system. This indicates that for every mJ/cm^2 of UV fluence, 0.0011 ppm of H_2O_2 is utilized under LPUV, while 0.0180 ppm of H_2O_2 is utilized for every mJ/cm^2 of UV fluence under KrCl*. Similar results were obtained from NDMA in LGW experiments. H_2O_2 concentration decreased from 10.02 ppm to 8.81 ppm over a UV fluence of 1000 mJ/cm^2, while H_2O_2 concentration decreased from 9.64 ppm to 8.95 ppm over a UV fluence of 120 mJ/cm^2 in the filtered KrCl* excimer system. This indicates that for every mJ/cm^2 of UV fluence, 0.0012 ppm of H_2O_2 is utilized under LPUV, while 0.0058 ppm of H_2O_2 is utilized for every mJ/cm^2 of UV fluence under KrCl*.

Both CBZ and NDMA experiments were conducted in the same water source, so the only variation in scavenging is due to the reaction rate of CBZ or NDMA with •OH. Because CBZ reacts with

297 •OH approximately 10x faster than NDMA, it is possible that its presence has a more profound
298 comparative impact on the caging effect of H_2O_2. UV irradiation upon H_2O_2 can result in the
299 formation of two •OH, however, some of it recombines to form H_2O_2. Since CBZ reacts faster
300 with H_2O_2, presumably less •OH was able to recombine and therefore we see a higher utilization
301 of H_2O_2 during the CBZ experiment. Similar effects were shown in Barrett et al. (1968), where
302 the presence of alcohol, which also reacts fast with •OH, slowed the recombination of H_2O_2. It
303 was hypothesized that the presence of alcohol in the caging region also prevented •OH from
304 reforming H_2O_2.

305 As shown in Table 3, the absorbance of the original SE (without spiking CBZ/NDMA nor H_2O_2)
306 at 254 nm is 0.028 cm^{-1} whereas the absorbance at 222 nm is 0.427 cm^{-1}, a 15-fold
307 increase. Using Eqn. 3, the fraction of photons being absorbed by H_2O_2 can be determined.

308 $$f_{H_2O_2} = \left(\frac{\alpha_{H_2O_2}}{\alpha_{Water\ Sample}}\right)\left(1 - 10^{-\alpha_{Water\ Sample} l}\right) \quad (3)$$

309 Where $f_{H_2O_2}$ is the fraction of photons absorbed by H_2O_2, $\alpha_{H_2O_2}$ is the absorbance of H_2O_2,
310 $\alpha_{Water\ Sample}$ is the absorbance of the water sample, and l is the pathlength.

311 Figure 4 shows the percentage of photons absorbed by CBZ, NDMA and H_2O_2 in SE experiments.
312 At 254 nm, 1.9% of the all photons absorbed by the water sample is by H_2O_2, whereas at 222 nm,
313 H_2O_2 absorbs 4.4% of all photons absorbed by the water. Despite increase in the fraction of H_2O_2
314 absorbed at 222 nm, AOP did not improve the degradation of CBZ in SE. This phenomenon was
315 not observed in a previous study with pCBA degradation in groundwater [44]. This might be due to
316 two reasons: 1) the composition of the different water types having different scavengers; 2) the
317 higher transmittance for groundwater compared to secondary effluent.

Table 4. CBZ and NDMA fluence-based degradation rate constants for filtered 222 nm excimer lamp and LPUV for both direct photolysis and UV/AOP (10ppm H_2O_2) in SE

	Direct Photolysis (cm^2/mJ)		AOP (10ppm H_2O_2) (cm^2/mJ)	
	Excimer 222F	**LPUV**	**Excimer 222F**	**LPUV**
CBZ	$(1.86 \pm 0.08) \times 10^{-2}$	$(2.98 \pm 0.27) \times 10^{-4}$	$(1.37 \pm 0.05) \times 10^{-2}$	$(3.19 \pm 0.16) \times 10^{-3}$
NDMA	$(1.45 \pm 0.88) \times 10^{-2}$	$(3.49 \pm 0.18) \times 10^{-3}$	$(1.77 \pm 0.26) \times 10^{-2}$	$(5.16 \pm 0.04) \times 10^{-3}$

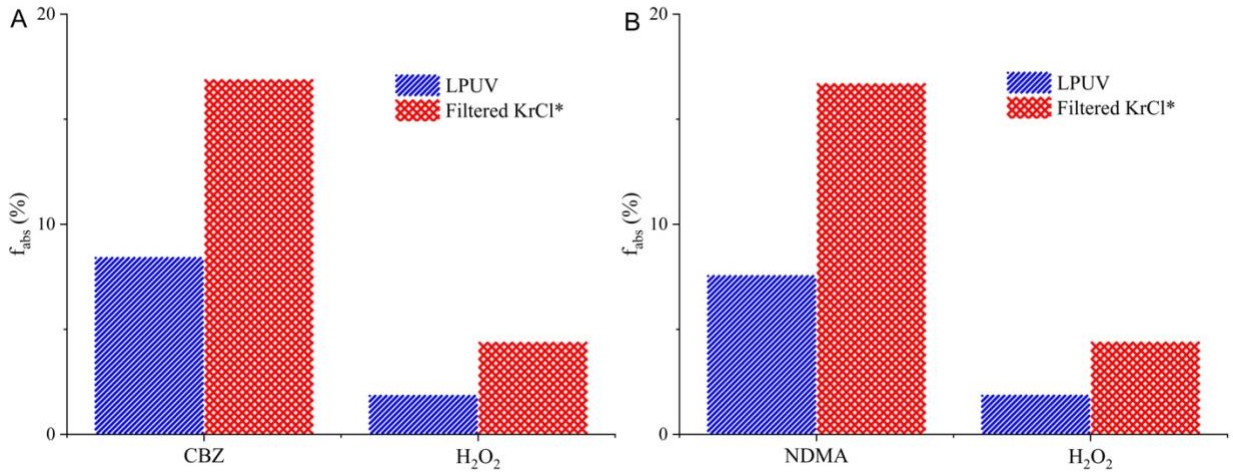

Figure 4. Percentage of light absorbed by A) CBZ and H_2O_2 in SE and B) NDMA and H_2O_2 in SE for under LPUV and Filtered KrCl*, respectively

3.3 UV/H_2O_2 Model Comparison

A model was developed to predict the degradation of CBZ and NDMA under different UV/AOP systems. The model is adapted from Rosenfeldt (2004). The rate of •OH formation accounts for both H_2O_2 and NO_3^- because NO_3^- adsorbs UV light strongly at wavelengths below 240 nm. The rate equation is shown in Eqn. 3.

$$r_{UV/H_2O_2}(\lambda) = E_{avg}[H_2O_2]\Phi_{H_2O_2}\varepsilon_{H_2O_2} + E_{avg}[NO_3^-]\Phi_{NO_3^-}\varepsilon_{NO_3^-} \quad (3)$$

Where $r_{UV/H_2O_2}(\lambda)$ is the rate of •OH formation rate $[M/s]$; E_{avg} is the average irradiance $[mw/cm^2]$, $[H_2O_2]$ and $[NO_3^-]$ are the concentration of H_2O_2 and NO_3^-, respectively, [M] ; $\Phi_{H_2O_2}$ and $\Phi_{NO_3^-}$ are the quantum yield of H_2O_2 and NO_3^-, respectively, $[mol/Es]$; $\varepsilon_{H_2O_2}$ and $\varepsilon_{NO_3^-}$ are the molar absorption coefficient of H_2O_2 and NO_3^-, respectively, $[1/M/cm]$.

As shown in Figure 5, the model underestimated the degradation of CBZ and NDMA at both 254 and 222 nm. Due to the nature of the water source, the exact constituents making up the water quality is not known, and only major parameters (TOC, Alkalinity, nitrate etc.) are accounted for in the model. Therefore, it is likely the model missed some of the scavengers and radical promoters present in the water. Because the model underestimated the degradation of both CBZ and NDMA, it is reasonable to conclude that the unknown radical promoters probably had a bigger impact than the unknown scavengers. For CBZ, the modelled fluence-based rate constant is 1.22×10^{-3} and $1.14 \times 10^{-2}\ cm^2/mJ$ for LPUV/AOP and KrCl*/AOP, respectively. The experimental fluence-based rate constant for CBZ, shown in Table 4, is 2.6 and 1.2 times higher than modelled rate for LPUV/AOP and KrCl*/AOP, respectively. For NDMA, the modelled fluence-based rate constant is 1.28×10^{-3} and $1.08 \times 10^{-2}\ cm^2/mJ$ for LPUV/AOP and KrCl*/AOP, respectively. The experimental fluence-based rate constant for NDMA, again shown in Table 4, is 4.0 and 1.6 times higher than modelled rate for LPUV/AOP and KrCl*/AOP, respectively. Although the model did not precisely predict the experimental degradation of CBZ nor NDMA, it represents the relative trends, and results between model and experiment differed by between 1.2-4 times.

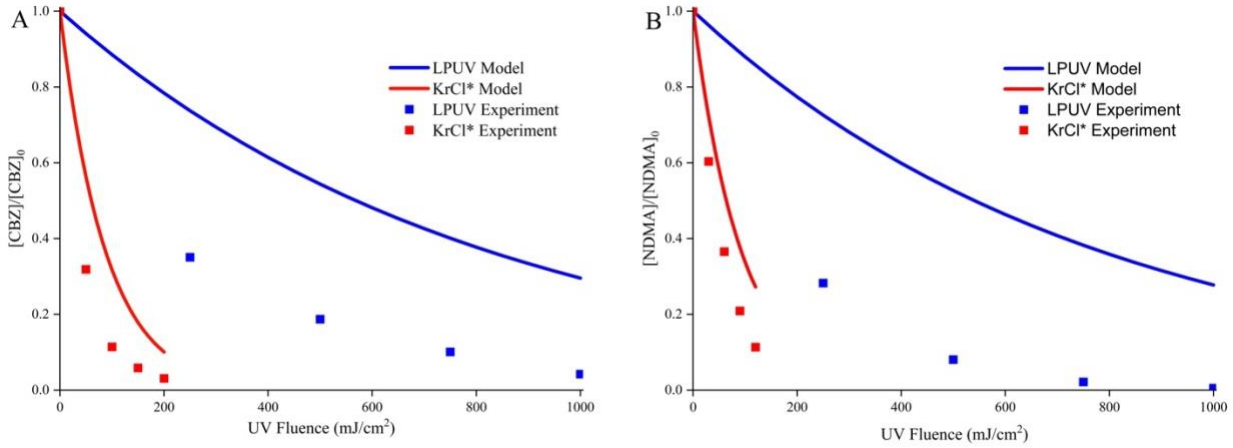

Figure 5. Modelling results of A) CBZ and B) NDMA for both LPUV and KrCl* AOP

3.4 Potential Environmental Impact and Implications

Despite filtered KrCl* excimer lamps emitting lower UV irradiation intensity compared to conventional LPUV, target contaminants were degraded more effectively for both UV direct and indirect photolysis. In SE, direct photolysis of CBZ under filtered KrCl* excimer was more effective than LPUV/AOP. This may be due to radicals formed from background water constituents that also absorb highly in the Far-UVC range. This can be beneficial to encourage radical generation from KrCl* lamps without external chemical inputs, especially for small treatment systems. Treatment plants would not only require less energy to degrade target contaminants, but potentially not utilize H_2O_2 during the treatment process, which would reduce the cost of quenching residual H_2O_2 and a H_2O_2 feeding. However, reactive species generated in-situ and contaminant degradation products/pathways were not directly probed for in this study. This finding of enhanced contaminant degradation in the absence of H_2O_2 due to in-situ reactive oxidant production warrants additional investigation, which is underway. Furthermore, the degradation products should be probed for any changes in solution toxicity that may outweigh the

benefits of utilizing KrCl* excimer lamps. This research only investigated CBZ and NDMA and found that the degradation efficiency improved significantly for both under filtered KrCl* excimer irradiation, despite different chemical structures, absorbances, and QY. However, that this may not be the case for other contaminants and further investigation must be conducted to confirm the UV degradation behavior of other chemicals, as well as the role of reactive species generated in-situ and associated degradation by-products.

Another factor that will affect the utilization of KrCl* excimer technology is high UV transmittance (UVT) water. Both CBZ and NDMA absorbed less than 20% of the photons entering the water matrix during the degradation process mainly due to the high absorbance by background water constituents. If UVT is improved, more photons can be utilized to degrade target contaminants.

Supporting Information

Supporting information related to this article can be found at [DOI here].

Chemical structure of carbamazepine and NDMA, hydrogen peroxide concentration and pH values for UV exposure experiments in both LGW and SE.

Acknowledgement

This work was supported by National Science Foundation-BiNational Science Foundation (NSF-BSF) Award CBET 1931168 to K.G.L and by the Discovery Learning Apprenticeship (DLA) Program at University of Colorado Boulder.

References

(1) Roback, S. L.; Ishida, K. P.; Chuang, Y.-H.; Zhang, Z.; Mitch, W. A.; Plumlee, M. H. Pilot UV-AOP Comparison of UV/Hydrogen Peroxide, UV/Free Chlorine, and UV/Monochloramine for the Removal of N -Nitrosodimethylamine (NDMA) and NDMA Precursors. *ACS ES&T Water* **2021**, *1* (2), 396–406. https://doi.org/10.1021/acsestwater.0c00155.

(2) Sharpless, C. M.; Linden, K. G. Experimental and Model Comparisons of Low- and Medium-Pressure Hg Lamps for the Direct and H2O2 Assisted UV Photodegradation of N-Nitrosodimethylamine in Simulated Drinking Water. *Environ Sci Technol* **2003**, *37* (9), 1933–1940. https://doi.org/10.1021/es025814p.

(3) Deng, J.; Shao, Y.; Gao, N.; Xia, S.; Tan, C.; Zhou, S.; Hu, X. Degradation of the Antiepileptic Drug Carbamazepine upon Different UV-Based Advanced Oxidation Processes in Water. *Chemical Engineering Journal* **2013**, *222*, 150–158. https://doi.org/10.1016/j.cej.2013.02.045.

(4) Vogna, D.; Marotta, R.; Andreozzi, R.; Napolitano, A.; D'Ischia, M. Kinetic and Chemical Assessment of the UV/H2O2 Treatment of Antiepileptic Drug Carbamazepine. *Chemosphere* **2004**, *54* (4), 497–505. https://doi.org/10.1016/S0045-6535(03)00757-4.

(5) Pereira, V. J.; Weinberg, H. S.; Linden, K. G.; Singer, P. C. UV Degradation Kinetics and Modeling of Pharmaceutical Compounds in Laboratory Grade and Surface Water via Direct and Indirect Photolysis at 254 Nm. *Environ Sci Technol* **2007**, *41* (5), 1682–1688. https://doi.org/10.1021/es061491b.

(6) Zhou, S.; Xia, Y.; Li, T.; Yao, T.; Shi, Z.; Zhu, S.; Gao, N. Degradation of Carbamazepine by UV/Chlorine Advanced Oxidation Process and Formation of Disinfection by-Products. *Environmental Science and Pollution Research* **2016**, *23* (16), 16448–16455. https://doi.org/10.1007/s11356-016-6823-x.

(7) Ikehata, K.; Wang-Staley, L.; Qu, X.; Li, Y. Treatment of Groundwater Contaminated with 1,4-Dioxane, Tetrahydrofuran, and Chlorinated Volatile Organic Compounds Using Advanced Oxidation Processes. *Ozone Sci Eng* **2016**, *38* (6), 413–424. https://doi.org/10.1080/01919512.2016.1198686.

(8) Lee, C. S.; Venkatesan, A. K.; Walker, H. W.; Gobler, C. J. Impact of Groundwater Quality and Associated Byproduct Formation during UV/Hydrogen Peroxide Treatment of 1,4-Dioxane. *Water Res* **2020**, *173*, 115534. https://doi.org/10.1016/j.watres.2020.115534.

(9) Wang, W. L.; Wu, Q. Y.; Li, Z. M.; Lu, Y.; Du, Y.; Wang, T.; Huang, N.; Hu, H. Y. Light-Emitting Diodes as an Emerging UV Source for UV/Chlorine Oxidation: Carbamazepine Degradation and Toxicity Changes. *Chemical Engineering Journal* **2017**, *310*, 148–156. https://doi.org/10.1016/j.cej.2016.10.097.

(10) Buonanno, M.; Welch, D.; Shuryak, I.; Brenner, D. J. Far-UVC Light (222 Nm) Efficiently and Safely Inactivates Airborne Human Coronaviruses. *Sci Rep* **2020**, *10* (1), 1–8. https://doi.org/10.1038/s41598-020-67211-2.

(11) Eadie, E.; Hiwar, W.; Fletcher, L.; Tidswell, E.; O'Mahoney, P.; Buonanno, M.; Welch, D.; Adamson, C. S.; Brenner, D. J.; Noakes, C.; Wood, K. Far-UVC (222 Nm) Efficiently Inactivates an Airborne Pathogen in a Room-Sized Chamber. *Scientific Reports 2022 12:1* **2022**, *12* (1), 1–9. https://doi.org/10.1038/s41598-022-08462-z.

(12) Buxton, G. v.; Greenstock, C. L.; Helman, W. P.; Ross, A. B. Critical Review of Rate Constants for Reactions of Hydrated Electrons, Hydrogen Atoms and Hydroxyl Radicals (·OH/·O−) in Aqueous Solution. *J Phys Chem Ref Data* **1988**, *17* (2), 513–886. https://doi.org/10.1063/1.555805.

(13) Wols, B. A.; Hofman-Caris, C. H. M. Review of Photochemical Reaction Constants of Organic Micropollutants Required for UV Advanced Oxidation Processes in Water. *Water Research*. Elsevier Ltd June 1, 2012, pp 2815–2827. https://doi.org/10.1016/j.watres.2012.03.036.

(14) Snyder, S. A.; Wert, E. C.; Lei, H. (Dawn); Westerhoff, P.; Yoon, Y. *Removal of EDCs and Pharmaceuticals in Drinking and Reuse Treatment Processes*; Denver, CO, 2007.

(15) Rosenfeldt, E. J.; Linden, K. G. Degradation of Endocrine Disrupting Chemicals Bisphenol A, Ethinyl Estradiol, and Estradiol during UV Photolysis and Advanced Oxidation Processes. *Environ Sci Technol* **2004**, *38* (20), 5476–5483. https://doi.org/10.1021/es035413p.

(16) Chuang, Y. H.; Chen, S.; Chinn, C. J.; Mitch, W. A. Comparing the UV/Monochloramine and UV/Free Chlorine Advanced Oxidation Processes (AOPs) to the UV/Hydrogen Peroxide AOP under Scenarios Relevant to Potable Reuse. *Environ Sci Technol* **2017**, *51* (23), 13859–13868. https://doi.org/10.1021/acs.est.7b03570.

(17) Zhang, Z.; Chuang, Y. H.; Szczuka, A.; Ishida, K. P.; Roback, S.; Plumlee, M. H.; Mitch, W. A. Pilot-Scale Evaluation of Oxidant Speciation, 1,4-Dioxane Degradation and Disinfection Byproduct Formation during UV/Hydrogen Peroxide, UV/Free Chlorine and

UV/Chloramines Advanced Oxidation Process Treatment for Potable Reuse. *Water Res* **2019**, *164*, 114939. https://doi.org/10.1016/j.watres.2019.114939.

(18) Ulliman, S. L.; McKay, G.; Rosario-Ortiz, F. L.; Linden, K. G. Low Levels of Iron Enhance UV/H2O2 Efficiency at Neutral PH. *Water Res* **2018**, *130*, 234–242. https://doi.org/10.1016/j.watres.2017.11.041.

(19) Vinge, S. L.; Shaheen, S. W.; Sharpless, C. M.; Linden, K. G. Nitrate with Benefits: Optimizing Radical Production during UV Water Treatment. *Environ Sci (Camb)* **2020**, *6* (4), 1163–1175. https://doi.org/10.1039/c9ew01138b.

(20) Dulova, N.; Kattel, E.; Kaur, B.; Trapido, M. UV-Induced Persulfate Oxidation of Organic Micropollutants in Water Matrices. *Ozone Sci Eng* **2020**, *42* (1), 13–23. https://doi.org/10.1080/01919512.2019.1599711.

(21) Li, W.; Patton, S.; Gleason, J. M.; Mezyk, S. P.; Ishida, K. P.; Liu, H. UV Photolysis of Chloramine and Persulfate for 1,4-Dioxane Removal in Reverse-Osmosis Permeate for Potable Water Reuse. *Environ Sci Technol* **2018**, *52* (11), 6417–6425. https://doi.org/10.1021/acs.est.7b06042.

(22) Miklos, D. B.; Remy, C.; Jekel, M.; Linden, K. G.; Drewes, J. E.; Hübner, U. Evaluation of Advanced Oxidation Processes for Water and Wastewater Treatment – A Critical Review. *Water Res* **2018**, *139*, 118–131. https://doi.org/10.1016/j.watres.2018.03.042.

(23) Kanakaraju, D.; Glass, B. D.; Oelgemöller, M. Advanced Oxidation Process-Mediated Removal of Pharmaceuticals from Water: A Review. *J Environ Manage* **2018**, *219*, 189–207. https://doi.org/10.1016/j.jenvman.2018.04.103.

(24) Ma, B.; Seyedi, S.; Wells, E.; McCarthy, D.; Crosbie, N.; Linden, K. G. Inactivation of Biofilm-Bound Bacterial Cells Using Irradiation across UVC Wavelengths. *Water Res* **2022**, *217* (December 2021), 118379. https://doi.org/10.1016/j.watres.2022.118379.

(25) Ma, B.; Gundy, P. M.; Gerba, C. P.; Sobsey, M. D.; Linden, K. G. UV Inactivation of SARS-CoV-2 across the UVC Spectrum: KrCl* Excimer, Mercury-Vapor, and Light-Emitting-Diode (LED) Sources. *Appl Environ Microbiol* **2021**, *87* (22). https://doi.org/10.1128/aem.01532-21.

(26) Blatchley, E. R.; Brenner, D. J.; Claus, H.; Cowan, T. E.; Linden, K. G.; Liu, Y.; Mao, T.; Park, S. J.; Piper, P. J.; Simons, R. M.; Sliney, D. H. Far UV-C Radiation: An Emerging Tool for Pandemic Control. *Crit Rev Environ Sci Technol* **2022**, *53* (6), 733–753. https://doi.org/10.1080/10643389.2022.2084315.

(27) Henderson, J.; Ma, B.; Cohen, M.; Dazey, J.; Meschke, J. S.; Linden, K. G. Field Study of Early Implementation of UV Sources and Their Relative Effectiveness for Public Health and Safety. *J Occup Environ Hyg* **2022**, *19* (9), 524–537. https://doi.org/10.1080/15459624.2022.2100404.

(28) Bolton, J. R.; Linden, K. G. Standardization of Methods for Fluence (UV Dose) Determination in Bench-Scale UV Experiments. *Journal of Environmental Engineering* **2003**, *129* (3), 209–215. https://doi.org/10.1061/(ASCE)0733-9372(2003)129:3(209).

(29) Klassen, N. v.; Marchington, D.; McGowan, H. C. E. H2O2 Determination by the I3− Method and by KMnO4 Titration. *Anal Chem* **1994**, *66* (18), 2921–2925. https://doi.org/10.1021/ac00090a020.

(30) Shah, A. D.; Dai, N.; Mitch, W. A. Application of Ultraviolet, Ozone, and Advanced Oxidation Treatments to Washwaters to Destroy Nitrosamines, Nitramines, Amines, and Aldehydes Formed during Amine-Based Carbon Capture. *Environ Sci Technol* **2013**, *47* (6), 2799–2808. https://doi.org/10.1021/es304893m.

(31) Bolton, J. R.; Mayor-Smith, I.; Linden, K. G. Rethinking the Concepts of Fluence (UV Dose) and Fluence Rate: The Importance of Photon-Based Units - A Systemic Review. *Photochem Photobiol* **2015**, *91* (6), 1252–1262. https://doi.org/10.1111/php.12512.

(32) Dürr, H.; Bouas-Laurent, H. *Photochromism Molecules and Systems*; Elsevier Science, 2003. https://doi.org/https://doi.org/10.1016/B978-0-444-51322-9.X5000-3.

(33) Wan, D.; Kong, Y.; Selvinsimpson, S.; Luo, F.; Chen, Y. Effect of UV254 Disinfection on the Photoformation of Reactive Species from Effluent Organic Matter of Wastewater Treatment Plant. *Water Res* **2020**, *185*. https://doi.org/10.1016/j.watres.2020.116301.

(34) Weishaar, J. L.; Aiken, G. R.; Bergamaschi, B. A.; Fram, M. S.; Fujii, R.; Mopper, K. Evaluation of Specific Ultraviolet Absorbance as an Indicator of the Chemical Composition and Reactivity of Dissolved Organic Carbon. *Environ Sci Technol* **2003**, *37* (20), 4702–4708. https://doi.org/10.1021/es030360x.

(35) Storozhok, N. M.; Medyanik, N. Kinetics and Mechanism of Photoconversion of N-Substituted Amides of Salicylic Acid. In *Photochemistry and Photophysics - Fundamentals to Applications*; InTech, 2018. https://doi.org/10.5772/intechopen.76472.

(36) Paul, A.; Dziallas, C.; Zwirnmann, E.; Gjessing, E. T.; Grossart, H. P. UV Irradiation of Natural Organic Matter (NOM): Impact on Organic Carbon and Bacteria. *Aquat Sci* **2012**, *74* (3), 443–454. https://doi.org/10.1007/s00027-011-0239-y.

(37) Beck, S. E.; Hull, N. M.; Poepping, C.; Linden, K. G. Wavelength-Dependent Damage to Adenoviral Proteins Across the Germicidal UV Spectrum. *Environ Sci Technol* **2018**, *52* (1), 223–229. https://doi.org/10.1021/acs.est.7b04602.

(38) Beck, S. E.; Rodriguez, R. A.; Linden, K. G.; Hargy, T. M.; Larason, T. C.; Wright, H. B. Wavelength Dependent UV Inactivation and DNA Damage of Adenovirus as Measured by Cell Culture Infectivity and Long Range Quantitative PCR. *Environ Sci Technol* **2014**, *48* (1), 591–598. https://doi.org/10.1021/es403850b.

(39) Pathak H Fellman, M. J. Activating and Fluorescent Wave-Lengths of Furocoumarins: Psoralens. *Nature* **1960**, 382–383.

(40) Rosario-Ortiz, F. L.; Canonica, S. Probe Compounds to Assess the Photochemical Activity of Dissolved Organic Matter. *Environ Sci Technol* **2016**, *50* (23), 12532–12547. https://doi.org/10.1021/acs.est.6b02776.

(41) Lester, Y.; Sharpless, C. M.; Mamane, H.; Linden, K. G. Production of Photo-Oxidants by Dissolved Organic Matter during UV Water Treatment. *Environ Sci Technol* **2013**, *47* (20), 11726–11733. https://doi.org/10.1021/es402879x.

(42) Scholes, R. C. Emerging Investigator Series: Contributions of Reactive Nitrogen Species to Transformations of Organic Compounds in Water: A Critical Review. *Environ Sci Process Impacts* **2022**, 851–869. https://doi.org/10.1039/d2em00102k.

(43) Barrett, J.; Mansell, A. L.; Ratcliffe, R. J. M. Cage Effects in the Photolysis of Hydrogen Peroxide in Alcohol-Water Mixtures. *Chemical Communications (London)* **1968**, No. 1, 48–49. https://doi.org/https://doi.org/10.1039/C19680000048.

(44) Payne, E. M.; Liu, B.; Mullen, L.; Linden, K. G. UV 222 Nm Emission from KrCl∗ Excimer Lamps Greatly Improves Advanced Oxidation Performance in Water Treatment. *Environ Sci Technol Lett* **2022**, *9* (9), 779–785. https://doi.org/10.1021/acs.estlett.2c00472.